[25] A. F. Filippov, "Differential Equations with Discontinuous Righthand Sides," in *Mathematics and Its Applications*. Dordrecht, The Netherlands: Prentice-Hall, 1988.
[26] Y. J. Lootsma, A. J. van der Schaft, and M. K. Çamlıbel, "Uniqueness of solutions of relay systems," *Automatica*, vol. 35, no. 3, pp. 467–478, 1999.
[27] W. P. M. H. Heemels, M. K. Çamlıbel, and J. M. Schumacher, "A time-stepping method for relay systems," in *Proc. 39th IEEE Conf. Decision and Control*, Sydney, Australia, 2000.
[28] J. C. Willems, "Dissipative dynamical systems," *Arch. Rational Mech. Anal.*, vol. 45, no. 5, pp. 321–393, 1972.
[29] M. K. Çamlıbel, W. P. M. H. Heemels, and J. M. Schumacher, "Dynamical analysis of linear passive networks with diodes. Part II: Consistency of a time-stepping method," Eindhoven Univ. of Technology, Dept. of Elect. Eng., Measurement and Control Systems, Eindhoven, The Netherlands, Tech. Rep. 00 I/03, 2000.
[30] M. K. Çamlıbel, "Complementarity methods in the analysis of piecewise- linear dynamical systems," Ph.D. dissertation, Dep. of Econometrics and Operations Res., Tilburg Univ., The Netherlands, 2001.
[31] J. L. Willems, *Stability Theory of Dynamical Systems*. Camden, NJ: Nelson, 1970.
[32] A. Pazy, *Semigroups of Linear Operators and Applications to Partial Differential Equations*. New York: Springer-Verlag, 1983.
[33] H. Lütkepohl, *Handbook of Matrices*. New York: Wiley, 1996.

Using the Cyclostationary Properties of Chaotic Signals for Communications

T. L. Carroll

***Abstract*—Cyclostationary signals have an expectation value which varies periodically in time. Chaotic signals that have large components at some discrete frequencies in their power spectra can be cyclostationary. The cyclostationarity persists even if the discrete frequency components are removed from the chaotic signal, leaving a signal with a purely broad band frequency spectrum. In this brief, a communications system is created by modulating information onto the periodic parts of a chaotic signal and then removing the periodic parts from the frequency spectrum. At the receiver, the periodic parts of the spectrum are restored by means of a nonlinear operation. This system is demonstrated both in simulations and real circuits, and the performance of this system is measured in simulations. Finally, some of the reasons why such a scheme might be useful are discussed.**

***Index Terms*—Chaos, communication, cyclostationary.**

I. Introduction

Chaotic circuits are natural generators of broad-band signals, so there has been research into applying chaotic circuits to spread spectrum communications [1]–[13]. Most of these communications methods depend on having a synchronized chaotic receiver or at least some sort of information about the chaotic signal at the receiver. Difficulties in synchronizing chaotic receivers make most of these techniques impractical for multi-user communications systems. In addition, much research has focussed on the possible security of chaotic communications systems.

Manuscript received July 28, 2000; revised January 2, 2001. This paper was recommended by Associate Editor M. Di Bernardo.

The author is with the U.S. Naval Research Laboratory, Washington, DC 20375 USA.

Publisher Item Identifier S 1057-7122(02)02272-9.

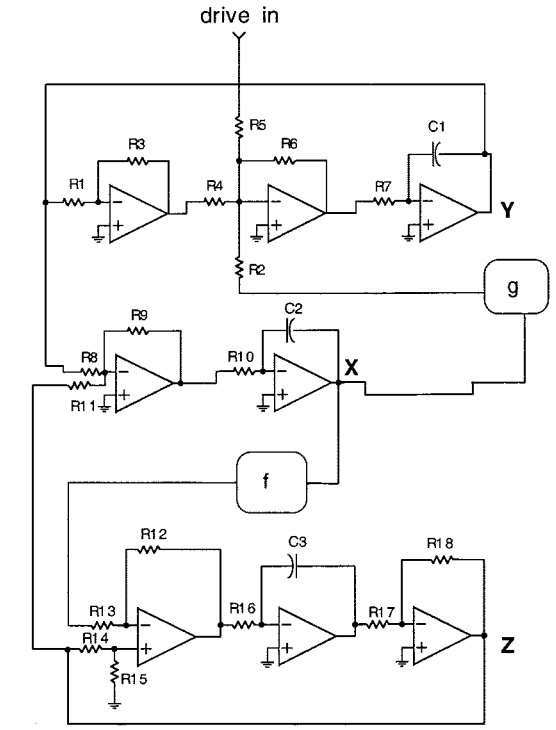

(a)

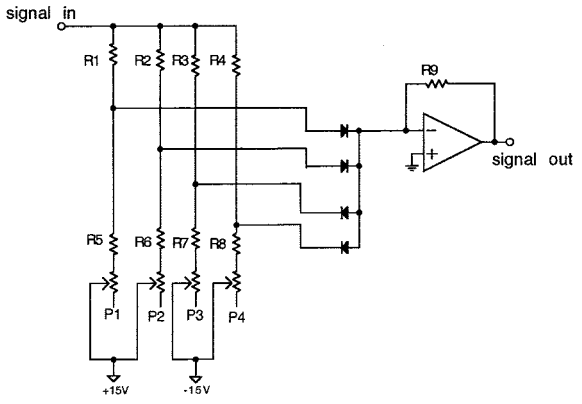

(b)

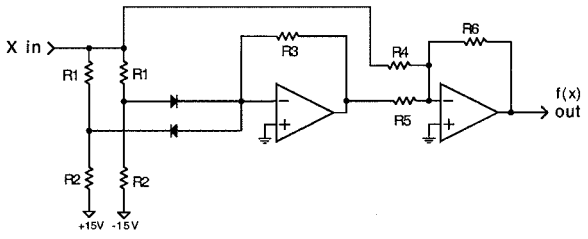

(c)

Fig. 1. (a). Chaotic Duffing circuit described by (1). $R1 = R3 = R4 = R5 = R6 = 10\ \text{k}\Omega, R2 = 39.2\ \text{k}\Omega, R7 = R10 = R12 = R13 = R14 = R16 = R17 = R18 = 100\ \text{k}\Omega, R8 = R9 = R18 = 1\ \text{M}\Omega, R15 = 5.2\ \text{k}\Omega, C1 = C2 = C3 = 0.001\ \mu\text{F}$. The box labeled f corresponds to the nonlinear function $f(x)$, while the box labeled g corresponds to the nonlinear function $g(x)$. All op amps are type 741 or equivalents. (b) Circuit used to generate the function $g(x)$. $R1 = R2 = R3 = R4 = R9 = 100\ \text{k}\Omega$. $R5 = R7 = 680\ \text{k}\Omega$. $R6 = R8 = 2\ \text{M}\Omega$. $P1 = P3 = 20\ \text{k}\Omega$ poteniometer. $P2 = P4 = 50\ \text{k}\Omega$ poteniometer. The diodes are all type 1N485B. The poteniometers are used to match different circuits to each other. The amplifier is type 741. (b) Schematic of circuit used to create $f(x)$ function. $R1 = 10\ \text{k}\Omega$. $R2 = 490\ \text{k}\Omega$. $R3 = 20\ \text{k}\Omega$. $R4 = R5 = R6 = 100\ \text{k}\Omega$.

There are still many applications for nonsecure spread spectrum communications. IEEE standard 802.11 sets aside certain frequency bands where no license is necessary to operate transmitters. Instead, regulations have been placed on the power spectra of the signals emitted by the transmitters so that the unlicensed signals do not interfere with other users. Essentially, the power spectra must be flat to within certain limits.

It is shown in this brief that some chaotic signals are cyclostationary [14], which means that the signal can be divided into a stationary part and a nonstationary part, with the expectation value of the nonstationary part varying periodically in time. The author demonstrates that the cyclostationary properties of chaotic signals may be used to encode information. One method for detection of a cyclostationarity in a signal is to calculate the spectral coherence, which is essentially the same as calculating the autocorrelation function of the Fourier transform of the signal, but substituting frequency shifts for time lags. If two frequencies are coherent (or phase locked), then the spectral coherence will show a peak when the first term in the spectral coherence calculation corresponds to the first frequency and the second term corresponds to the second frequency. By the Wiener–Khintchine theorem, the autocorrelation of the Fourier transform for zero frequency shift is just the Fourier transform of the signal squared, so simply squaring the chaotic signal may be enough to observe cyclostationarity. Also demonstrated is that some chaotic signals are cyclostationary. The power spectra of these signals have large components at certain discrete frequencies, but even after removing the parts of the signal at these frequencies, the cyclostationary property remains. The cyclostationarity may be used to recover a signal modulated onto the periodic parts of the original chaotic signal.

II. General Description

The method the author will demonstrate is as follows. Choose a nonautonomous chaotic circuit, or an autonomous circuit such as the Rossler system which has large peaks in its power spectrum. Information is modulated onto the narrow band frequency in the power spectrum, by some method such as phase modulation. If the chaotic attractor persists over a broad range of parameters, it may also be possible to use frequency or amplitude modulation. One (or more) chaotic signal from the chaotic circuit is chosen as a carrier signal, and the periodic components are suppressed, either through filtering or outright subtraction. Because the chaotic signal is cyclostationary, the periodic parts are still present in the statistical properties of the chaotic signal, so at the receiver the periodic components are restored by some nonlinear operation, such as squaring the chaotic carrier signal. The phase and other characteristics of the periodic component may then be extracted from the chaotic carrier after the nonlinear operation. Acronyms seem to be very popular in this field, so I will call the method presented here "chaos cyclostationary keying" (CCK).

When a binary phase modulation is used on the periodic component of the chaotic signal, CCK is in essence binary phase shift keying (BPSK) except that the narrow band phase modulated signal has been encoded on a chaotic signal for transmission. The properties of CCK will be similar to BPSK, except that there is some loss of performance when the periodic signal is converted to chaos and back.

III. Duffing Circuit Experiments

A. Transmitter

The first experiments were conducted with a circuit that is similar to the Duffing system [15]. Fig. 1 is a schematic of this circuit, while Fig. 2 is a plot of an attractor from this circuit. This same circuit was used in previous work [16], [17], although in the previous work there was an error in the equations describing the circuit. The set of equations describing the circuit are

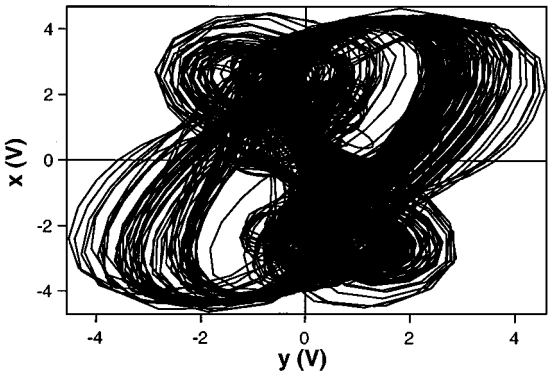

Fig. 2. Attractor for the circuit of Fig. 1.

$$\begin{aligned}
\frac{dx}{dt} &= \alpha[y - z] \\
\frac{dy}{dt} &= \alpha[-0.1y - g(x) + 2\sin(\theta)] \\
\frac{dz}{dt} &= \alpha[f(x) - 0.1z] \\
\frac{d\theta}{dt} &= \omega + \phi_d \\
g(x) &= \left\{ \begin{array}{ll} 2x + 3.8 & x < -2.6 \\ x + 1.2 & -2.6 \le x < -1.2 \\ 0 & -1.2 \le x \le 1.2 \\ x - 1.2 & 1.2 < x \le 2.6 \\ 2x - 3.8 & x > 2.6 \end{array} \right\} \\
f(x) &= \left\{ \begin{array}{ll} x + 2 & x < -1 \\ -x & -1 \le x \le 1 \\ x - 2 & x > 1 \end{array} \right\}. \qquad (1)
\end{aligned}$$

The periodic driving signal is θ, with a frequency $\omega = (2\pi) \times 780$ rad/sec, and the phase of the driving signal is given by ϕ. The time constant α was set to 10^4 to simulate the same time scale as the circuit. The boxes labeled f and g were piecewise linear diode function generators whose outputs were described by $f(x)$ and $g(x)$ in (1). The power spectrum of the y signal from the circuit is shown in Fig. 3(a).

The power spectrum of the y signal in Fig. 3(a) shows large narrow-band components at the driving frequency of 780 Hz and at its harmonics. These narrow-band components were removed by subtraction. The component at 780 Hz was removed by taking the 780-Hz driving signal, passing it through an all-pass filter to generate the appropriate phase shift, using an amplifier to scale the phase shifted signal to the proper amplitude, and subtracting from the y signal. The main nonlinearity in this circuit is cubic, so the narrowband component at the second harmonic frequency of 1560 Hz was not large compared to the broad-band background, but this harmonic was also removed to insure that the received signal was not simply caused by some small term at this frequency.

A periodic signal at the second harmonic frequency of 1560 Hz was generated by filtering the y signal with a fourth-order bandpass filter centered at 1560 Hz and then using this signal to drive a phase-locked loop. The phase-locked loop was constructed from a sample and hold amplifier, an Intersil ICL8038 function generator chip, and a low pass filter. The phase-locked loop output was phase shifted and scaled by an appropriate amount and subtracted from the y signal to generate the y_f signal, which is the y signal with the narrow band parts removed. The power spectrum of the y_f signal is shown in Fig. 3(b). For the circuit, only the driving frequency and the second harmonic were removed,

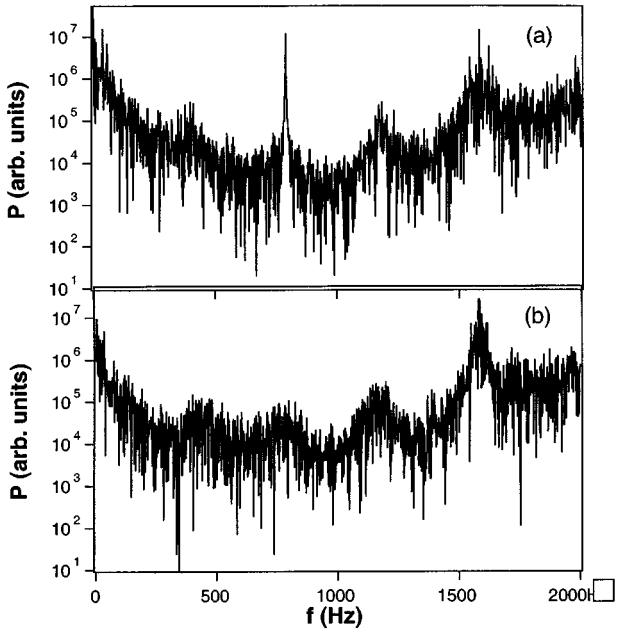

Fig. 3. (a) Power spectrum of the y signal from the circuit of Fig. 1. (b) Power spectrum of the y signal from the circuit of Fig. 1 after the periodic parts have been removed.

although in the simulation shown later, more of the harmonics were removed. The y_f signal could be transmitted directly or modulated onto a carrier signal for transmission.

B. Cyclostationarity

Although the narrow-band components of the y signal have been removed, they may still be reconstructed from the broad-band part of the chaotic y signal. The concepts behind the signal reconstruction may be explained simply by looking at a sum of periodic signals. Consider a sum of 2 sine waves, $s = \sin(f1) + \sin(f2)$. If we perform a nonlinear operation on these signals, such as cubing (in this brief, cubing is used as an example because the circuit described here has a cubic nonlinearity), then sum and difference frequencies are produced as the sine waves are modulated together: $s^3 \propto \sin(f1) - \sin(3f1) - \sin(f1\text{-}2f2) + \cdots$. It is then possible to remove terms that contain only factors of $f1$, such as $\sin(f1)$ or $\sin(3f1)$ etc., to produce the signal s_f^3.

At the receiver, another nonlinear operation may be performed on the received signal, such as squaring, to produce $(s_f^3)^2 \propto \cos(2f1) + \cos(4f1) +$ other terms. Terms containing only $f1$ have been restored, so it is possible to detect variations in the phase of the signal at frequency $f1$.

The actual chaotic y signal contains many frequencies, but because of the nonlinearities in the chaotic circuit, the frequencies are mixed together as described above. There are detailed discussions of cyclostationarity in the literature [14], [18], but a detailed understanding is not required to understand the signal recovery method here.

Cyclostationarity may be detected in a signal by calculating the autocorrelation of the power spectrum [18]. If $x(t)$ is a signal and $X(f)$ is its Fourier transform, then the autocorrelation of the power spectrum is

$$\Gamma(f) = \frac{\int_{-\infty}^{\infty} X(f)X^*(f-\phi)\,d\phi}{\int_{-\infty}^{\infty} X(\phi)X^*(\phi)\,d\phi}. \tag{2}$$

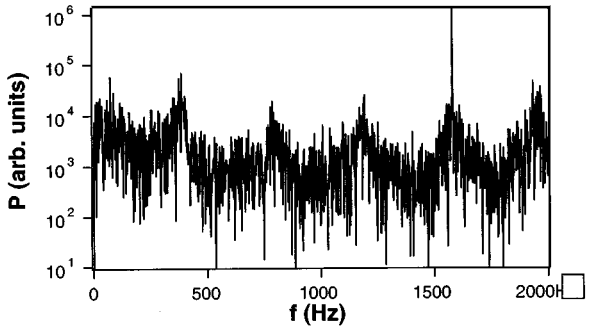

Fig. 4. Power spectrum of the signal $(y_f)^2$ (y_f is the y signal from the circuit of Fig. 1 with the periodic parts removed).

A large cross correlation at a particular frequency in the Fourier spectrum indicates the presence of cyclostationarity (an analogous result holds for discrete signals). From the Wiener–Khintchine theorem, one may equivalently simply take the square of $x(t)$, and search for large components at discrete frequencies.

C. Signal Detection

In order to detect information on the signal y_f from the circuit of Fig. 1, the signal is squared. The power spectrum of $(y_f)^2$ is shown in Fig. 4. The narrow-band component at 1560 Hz is obvious in the power spectrum. Cubing y_f would produce a signal at the driving frequency of 780 Hz, but the signal-to-noise ratio (SNR) of the narrow-band component was not as good as when y_f was squared.

The signal $(y_f)^2$ was then filtered with a second-order bandpass filter with a center frequency of 1560 Hz prior to phase detection. In order to detect the phase of the filtered $(y_f)^2$ at 1560 Hz, a local oscillator was also run at 1560 Hz (there was some slight mismatch between oscillator frequencies in the transmitter and receiver, but a small mismatch will not greatly affect the results). The signal $(y_f)^2$ was an input for a sample and hold amplifier, which was strobed with the 1560-Hz signal from the local oscillator. The output of the sample and hold amplifier was low pass filtered to form the phase error signal Δ.

The simplest way to encode information onto the chaotic signal y_f was to modulate the phase of the periodic signal driving the circuit (essentially a form of BPSK). We know that the signal in the detector will be squared, so using the identity $\sin(\omega t+\phi)^2 = 0.5(1-\cos(2\omega t+2\omega\phi))$ tells us that the largest possible signal at the receiver will come when the periodic driving signal phase is modulated by $\pm 45^\circ$ (a phase shift of 90° in the transmitter is equivalent to a phase shift of 180° in the receiver). Fig. 5(a) shows the phase modulation signal in the transmitter, while 5(b) shows the phase error signal Δ from the receiver when the periodic driving signal at the transmitter is phase modulated by $\pm 45^\circ$ at a frequency of 10 Hz. Fig. 5 shows that it is possible to detect the phase of the periodic driving signal even though the periodic parts of the transmitted signal have been removed. The phase error signal could also be used to phase synchronize a periodic oscillator in the receiver in order to build a synchronized chaotic response circuit. In a later section of this brief, numerical simulations will be performed in order to measure the bit error rate of this communications system.

IV. Rossler Circuit Experiments

The Duffing circuit used above was nonautonomous. Some autonomous chaotic circuits have strong narrow-band components in their frequency spectra, so it should be possible to remove the periodic parts and still recover their phase, as with the nonautonomous circuit.

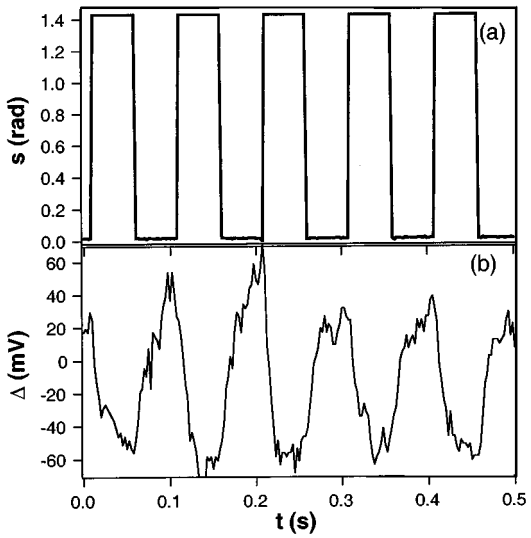

Fig. 5. (a) Phase-modulation signal s used to modulate the periodic signal driving the circuit of Fig. 1. The phase-modulation rate is 20 Hz. (b) Phase-error signal Δ measured at the receiver.

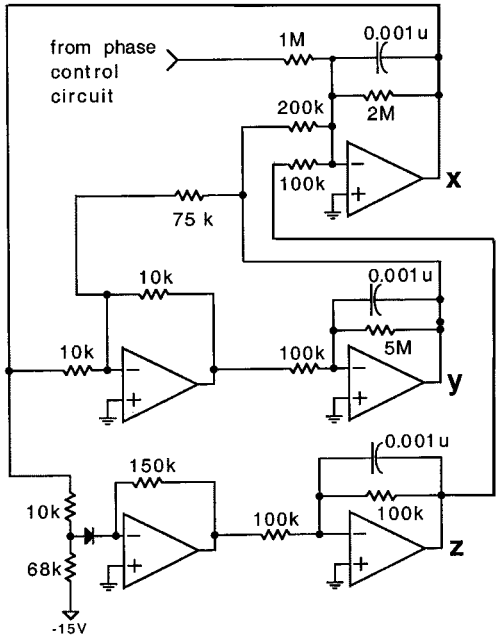

Fig. 6. PLR circuit described by (5).

To test this idea, the piecewise-linear Rossler (PLR) circuit shown in Fig. 6 was used [19]. The PLR circuit may be described by the equations

$$\begin{aligned}\frac{dx}{dt} &= -\alpha[0.05x + 0.5y + z + c_\phi(A\sin(\omega_c t + \phi) - x)] \\ \frac{dy}{dt} &= -\alpha[-x - 0.11y] \\ \frac{dz}{dt} &= -\alpha[z + g(x)] \\ g(x) &= \begin{cases} 0 & x \le 3 \\ 15(x-3) & x > 3 \end{cases} \end{aligned} \tag{3}$$

where $\alpha = 10^4$ s^{-1}, the phase control coupling constant $c_\phi = 0.025, A = 3.15, \phi$ is varied in order to control the PLR circuit phase, and ω_c is set to the peak frequency in the PLR spectrum, which is 1.16 kHz. The term multiplied by c_ϕ in the PLR circuit is

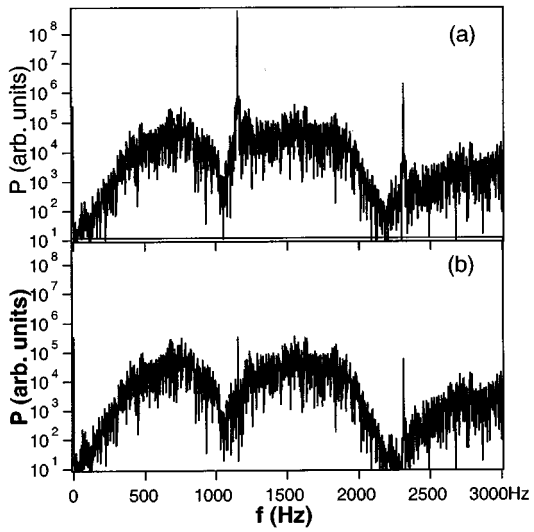

Fig. 7. (a) Power spectrum of the x signal from the circuit of Fig. 6. (b) Power spectrum of the x signal from Fig. 6 when the periodic parts have been supressed by filtering.

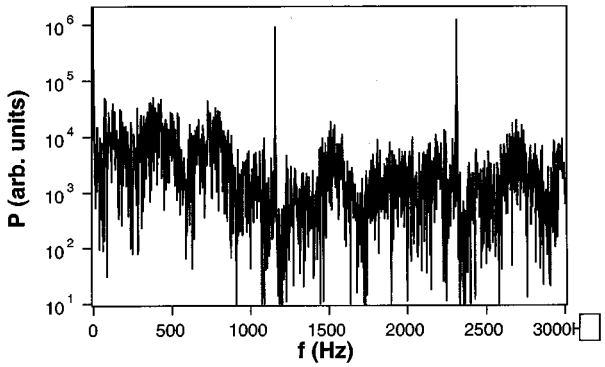

Fig. 8. Power spectrum of the signal $(x_f)^2$ (x_f is the y signal from the circuit of Fig. 6 with the periodic parts supressed).

used to control the phase of the narrow-band component of the PLR frequency spectrum through phase synchronization [20]. Fig. 7(a) shows the power spectrum of the x signal from the PLR circuit.

Rather than using phase-locked loops, the periodic components were removed from the PLR x signal by filtering and subtraction. Second-order bandpass filters were used to isolate the components of the PLR x signal at 1.16 and 2.32 kHz, and the outputs of the bandpass filters were subtracted from the x signal to produce the signal x_f. The power spectrum of x_f is shown in Fig. 7(b). There is still some evidence of narrow-band signals at 1.16 and 2.32 kHz, but their amplitude is down by a factor of 1000. One advantage of using filters instead of phase-locked loops to remove the periodic components is that the filter will still remove the periodic component if its amplitude changes, allowing for amplitude modulation of the periodic component. The phase-locked loop, on the other hand, compensates better for small variations in the frequency of the periodic component.

Fig. 8 shows the power spectrum of $(x_f)^2$. In this case, there are peaks at both the fundamental of 1.16 kHz and the second harmonic of 2.32 kHz, possibly because these signals were not completely removed from x_f. Once again, the phase of the second harmonic at 2.32 kHz is detected when the phase of the 1.16-kHz frequency in PLR circuit is varied by using phase synchronization. Fig. 9(a) shows the phase-modulation signal, while Fig. 9(b) shows the phase–error signal Δ, demonstrating that it is possible to recover the phase of the periodic

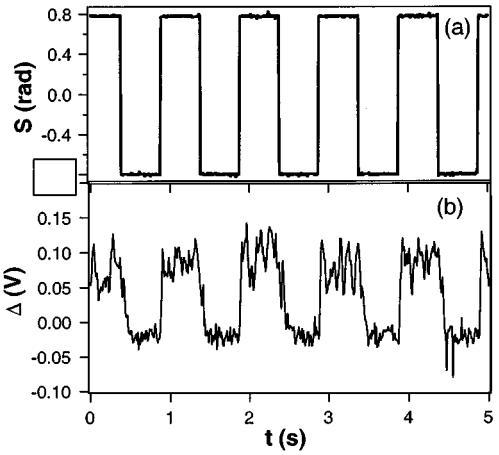

Fig. 9. (a) Phase-modulation signal s used to modulate the phase of the periodic part of the chaotic signal from the PLR circuit of Fig. 6. The phase-modulation rate was 1 Hz. (b) Phase error signal detected at the receiver.

TABLE I
AMPLITUDES a_I AND PHASES ϕ_I OF THE DRIVING FREQUENCY ($i = 1$) AND ITS NEXT FOUR HARMONICS ($i = 2$–5) FROM THE y SIGNAL IN THE SIMULATION OF (1). THESE CONSTANTS WERE DETERMINED FROM THE FOURIER TRANSFORM OF A LONG-TIME SERIES.

i	a_i	ϕ_i
1	0.6516	0.0943
2	0.1407	0.3741
3	0.2027	1.9559
4	0.0662	0.7032
5	0.0716	2.4081

part of a chaotic signal from an autonomous chaotic circuit when the periodic part has been suppressed. In Fig. 9, the phase is modulated at a frequency of 1 Hz.

V. SIMULATIONS

When used as a communications system, it is most likely that a whole set of nonautonomous circuits would be used, with each circuit having a different drive frequency. It would be possible to build many copies of the same circuit and simply rescale the time constants (α in (1)) so that every transmitter-receiver pair operated at a slightly different frequency. This method would amount to using frequency division multiplexing with binary phase-shift keying (BPSK), except that the periodic carrier signal is spread with the chaos to prevent it from interfering with other transmitters.

The circuit described by (1) was numerically simulated (using a Runge–Kutta integrator with a time step of 5×10^{-5} s.) to determine its bit error performance when a simple phase shifting encoding technique was used. For the simulation, the drive frequency and the next 4 harmonics were subtracted from the y signal to generate the transmitted signal y_s

$$y_s = y - \sum_{i=1}^{5} a_i \sin(i\theta - \phi_i) + \eta \tag{4}$$

where η is an additive noise term, θ is defined in (1), and the parameters a_I and ϕ_I are defined in Table I. An information signal was encoded onto the chaotic signal by varying the drive phase ϕ_d between ± 1 radian at a frequency of 20 Hz.

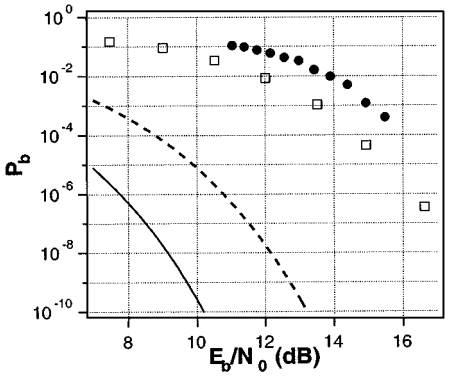

Fig. 10. Circles show the probability of bit error P_b as a function of (energy per bit)/(noise power spectral density) E_b/N_0 for chaos cyclostationary keying (CCK) with added white Gaussian noise. The solid line is the probability of bit error for BPSK, the dotted line is P_b for PSK with phases $\pm 45^\circ$, and the squares are P_b for DCSK.

At the simulated receiver, y_s was squared and filtered with a bandpass filter with a center frequency of 1560 Hz:

$$\begin{aligned} \frac{du}{dt} &= \frac{-y_s^2}{r_1 c} - \frac{u}{r_2 c} + v \\ \frac{dv}{dt} &= \frac{-u(r_1 + r_3)}{r_1 r_2 r_3 c^2} \end{aligned} \tag{5}$$

where u was the filter output and $r_1 = 102\,000\ \Omega$, $r_2 = 204\,000\ \Omega$, and $r_3 = 513\ \Omega$.

The next step in the receiver was to determine the phase of u. The signal s_u was generated, where $s_u = 1$ for $u \geq 0$ and $s_u = -1$ for $u < 0$. This signal s_u was used to strobe a sinusoidal signal at 1560 Hz

$$\begin{aligned} \frac{d\theta_r}{dt} &= \omega \\ \delta &= \sin(2\theta_r)|_{s_u = 0\uparrow} \\ \frac{d\Delta}{dt} &= 1000(\delta - \Delta) \end{aligned} \tag{6}$$

where ω is the same as in (1) and δ is produced by sampling $\sin(\theta_r)$ when s_u crosses zero in the positive direction. The final phase error signal is Δ, which is the low pass filtered version of δ. The value of Δ is set to 0 at the start of each bit and the final value of Δ at the end of each bit is used to determine whether a binary 1 or 0 was sent.

A. Comparison to BPSK

Fig. 10 shows the probability of bit error P_b as a function of (bit energy)/(noise power spectral density) when (1) is used to simulate a transmitter and the added noise is Gaussian white noise. The bit-error performance is not as good as simple BPSK, but that is to be expected, as producing the chaos and detecting the periodic signal will have some effect on performance. The transmitted signal will interfere less with other signals than a periodic BPSK signal will, so something is gained by using chaos. The performance shown in Fig. 10 is probably not ideal since the bit-error probability shown here does depend on the bandpass filter in the receiver, which is not ideal.

For comparison, the solid line in Fig. 10 shows the bit error probability of BPSK, while the dotted line shows the probability of bit error for a PSK signal with a phase shift of $\pm 45^\circ$. These lines are calculated from analytic formulas [21], so they are ideal. The squares in Fig. 10 are the calculated bit-error rate for differential chaos shift keying (DCSK) [22]–[24], which is another asynchronous chaotic communication method. The DCSK curve appears slightly better, but it should be noted that the performance of DCSK will be worse for signal to noise ratios less than 0 dB [24]. For the DCSK data in Fig. 10, the

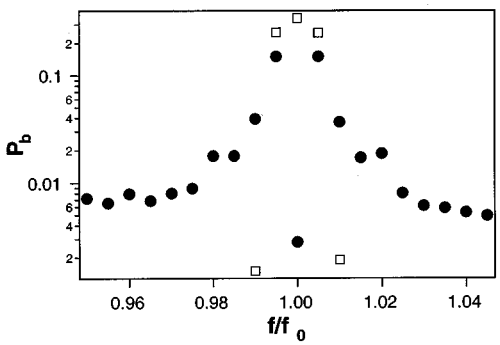

Fig. 11. Probability of bit error P_b as a function of interference frequency (normalized by driving frequency). The dark circles are for interference from another CCK transmitter, while the open squares are for interference from a purely sinusoidal signal.

SNR corresponding to E_b/N_0 =16 dB is estimated to be + 0.69 dB [24]; for the CCK data in Fig. 10, the SNR for E_b/N_0 =16 dB was −10.9 dB (with a bit length of 0.05 s), although, as with DCSK, the bit error probability curve will shift for different bit lengths, so CCK is not noise robust under the definition of Abel [24]. CCK is not noise robust because the noise is also squared when the received signal is squared.

Other transmitter-receiver pairs could be added by using frequency division multiplexing. The effect of interference from another transmitter with the same power is shown in Fig. 11. The solid circles show the probability of bit error P_b when a signal from a second Duffing system has been added to the chaotic carrier signal. The interfering signal comes from a Duffing system that is identical to (1) except that the time constant α and the frequency ω have been multiplied by a constant. The x axis in Fig. 11 shows the driving frequency for the interfering signal divided by the driving frequency for the chaotic system producing the carrier signal. The frequency range of this plot is limited to values close to 1.0 because the bandpass filter in the receiver supresses interfering signals outside of this range.

The interference acts like a small constant noise signal outside the 20-Hz bandwidth of the information signal, and only causes significant interference when the interference is within the information bandwidth. The bandwidth efficiency of this chaotic communications method should be about the same as for BPSK.

Periodic interference will also affect the chaotic carrier signal. Also shown in Fig. 11 (open squares) is the bit error rate caused by a sinusoidal interference signal with the same power as the chaotic carrier signal. The interference from a sinusoidal signal is negligible outside of the 20-Hz information bandwidth. The effect of sinusoidal interference could be further reduced by filtering the received signal with a notch filter which removes signal components at the driving frequency. The peak power in the chaotic carrier power spectrum is a factor of 10 less than the peak power in a sinusoidal signal of the same total power; a better choice of chaotic circuit could reduce this ratio even more.

VI. Conclusion

It is possible to use the cyclostationarity properties of chaos to generate a broad-band carrier signal which has performance characteristics similar to BPSK, with only a small loss involved in converting the signal into chaos and back CCK. The advantage of the chaotic signal is that it has a relatively flat spectrum, and, therefore, will not interfere with other signals, making it useful for unlicensed communications applications. There are other methods for producing broad-spectrum communications signals, but CCK is very simple, and therefore, potentially very inexpensive.

References

[1] K. M. Cuomo, A. V. Oppenheim, and S. H. Strogatz, "Synchronization of Lorenz-based chaotic circuits with applications to communications," *IEEE Trans. Circuits Syst. II*, vol. 40, pp. 626–633, Oct. 1993.

[2] L. O. Chua, L. Kocarev, K. Eckart, and M. Itoh, "Experimental chaos synchronization in Chua's circuit," *Int. J. Bifurcations Chaos*, vol. 2, no. 9, pp. 705–708, 1992.

[3] T. L. Carroll, "Spread spectrum sequences from unstable periodic orbits," *IEEE Trans. Circuits Syst. I*, vol. 47, pp. 443–447, Apr. 1999.

[4] H. Dedieu, M. P. Kennedy, and M. Hasler, "Chaos shift keying: Modulation and demodulation of a chaotic carrier using self synchronizing Chua's circuits," *IEEE Trans. Circuits Syst. II*, vol. 40, pp. 634–642, Oct. 1993.

[5] S. Hayes, C. Grebogi, E. Ott, and A. Mark, "Experimental control of chaos for communication," *Phys. Rev. Lett.*, vol. 73, no. 13, pp. 1781–1784, 1994.

[6] L. Kocarev and U. Parlitz, "General approach for chaotic synchronization with applications to communication," *Phys. Rev. Lett.*, vol. 74, no. 9, pp. 5028–5031, 1995.

[7] G. Kolumban, M. P. Kennedy, and L. O. Chua, "The role of synchronization in digital communications using chaos—Part I: Fundamentals of digital communications," *IEEE Trans. Circuits Syst. I*, vol. 44, pp. 927–935, Oct. 1997.

[8] G. Mazzini, G. Setti, and R. Rovatti, "Chaotic complex spreading sequences for asynchronous DS-CDMA—Part I: System modeling and results," *IEEE Trans. Circuits Syst. I*, vol. 44, pp. 937–947, Oct. 1997.

[9] K. Murali and M. Lakshmanan, "Transmission of signals by synchronization in a chaotic Van der Pol-Duffing oscillator," *Phys. Rev. E*, vol. 48, no. 9, pp. 1624–1626, 1993.

[10] U. Parlitz, L. Kocarev, T. Stojanovski, and H. Prekel, "Encoding messages using chaotic synchronization," *Phys. Rev. E*, vol. 53, no. 5, pp. 4351–4361, 1996.

[11] E. Rosa, S. Hayes, and C. Grebogi, "Noise filtering in communication with chaos," *Phys. Rev. Lett.*, vol. 78, no. 7, pp. 1247–1250, 1997.

[12] N. F. Rulkov and L. Tsimring, "Communication with chaos over band-limited channels," *I. J. Circuit Theory Applicat.*, vol. 27, no. 6, pp. 555–567, 1999.

[13] K. M. Short, "Steps toward unmasking secure communications," *Int. J. Bifurcations Chaos*, vol. 4, no. 8, pp. 959–977, 1994.

[14] A. Papoulis, *Probability, Random Variables, and Stochastic Processes*. New York: McGraw-Hill, 1991.

[15] C. Hayashi, *Nonlinear Oscillations in Physical Systems*. Princeton, NJ: Princeton Univ. Press, 1964.

[16] T. L. Carroll and L. M. Pecora, "Synchronizing nonautonomous chaotic circuits," *IEEE Trans. Circuits Syst. II*, vol. 40, pp. 646–649, Oct. 1993.

[17] T. L. Carroll, "Communicating using filtered synchronized chaotic signals," *IEEE Trans. Circuits Syst. I*, vol. 42, pp. 105–110, Feb. 1995.

[18] M. Benidir, "Theoretical foundations of higher-order statistical processing and polyspectra," in *Higher-Order Statistical Signal Processing*, B. Boashash, E. J. Powers, and A. M. Zoubir, Eds, Singapore: Wiley, 1995, pp. 27–88.

[19] T. L. Carroll, "A simple circuit for demonstrating regular and synchronized chaos," *Amer. J. Phys.*, vol. 63, no. 4, pp. 377–379, 1995.

[20] A. S. Pikovsky, M. G. Rosenblum, G. V. Osipov, and J. Kurths, "Phase synchronization of chaotic oscillators by external driving," *Physica D*, vol. 104, no. 3–4, pp. 219–238, 1997.

[21] B. Sklar, *Digital Communications, Fundamentals and Applications*. Englewood Cliffs, NJ: Prentice-Hall, 1988.

[22] G. Kolumban, "Basis function description of chaotic modulation schemes," presented at the Conf. on Nonlinear Dynamics of Electronic Systems, Catania, Italy, 2000.

[23] M. P. Kennedy, G. Kolumban, and G. Kis, "Chaotic modulation for robust digital communications over multipath channels," *Int. J. Bifurcations Chaos Appl. Sci.Eng.*, vol. 10, no. 4, pp. 695–718, 2000.

[24] A. Abel, W. Schwartz, and M. Goetz, "Noise performance of chaotic communication systems," *IEEE Trans. Circuits Syst. I*, Dec. 2000.